V European Conference on Computational Fluid Dynamics
ECCOMAS CFD 2010
J. C. F. Pereira and A. Sequeira (Eds)
Lisbon, Portugal, 14–17 June 2010

HIGH REYNOLDS NUMBER TRANSITION EXPERIMENTS IN THE ETW TEST FACILITY WITH THE PATHFINDER MODEL

Jean Perraud[*], Itham Salah El Din[†], Geza Schrauf[§], Ardeshir Hanifi[‡], Raffaele Donelli[**], Stefan Hein[††], Uwe Fey[††], Yasuhiro Egami[††], Thomas Streit[§§]

[*]ONERA,
Toulouse, 31055 France
e-mail: jean.perraud@onera.fr
[††] ONERA,
Chalais-Meudon, 92320 France
e-mail: itham.Salah_el_din@onera.fr
[§]Airbus,
D-28199 Bremen, Germany
e-mail: Geza.Schrauf@airbus.com
[‡]FOI,
SE-164 90, Stockholm, Sweden
e-mail: Ardeshir.Hanifi@foi.se
[**]CIRA,
Capua, 81043 Italy
e-mail: mailto:r.donelli@cira.it
[††]DLR,
D-37073 Göttingen, Germany
e-mail: Stefan.Hein@dlr.de, uwe.fey@dlr.de, mailto:y.egami@coe.mech.nagoya-u.ac.jp
[§§]DLR,
D-38108 Braunschweig, Germany
e-mail: th.streit@dlr.de

Key words: Laminar-turbulent transition; ETW; Natural Laminar Flow

Abstract: *The Pathfinder model was designed in the course of the TELFONA European Research Project as a calibration tool to evaluate the transonic, cryogenic ETW facility for laminar flow testing, and assess the possibility for studies of NLF or HLF wings in ETW. The Pathfinder wing is a simplified, low taper, swept wing with an optimized profile allowing almost linear evolution of the N-factors in a wide range of flow conditions, especially designed for a precise estimation of transition N-factors. Temperature sensitive paint is used to allow optical detection of the transition location, and a series of pressure taps is used for measuring the pressure distribution. This general paper will cover model design, pre-test numerical evaluation, instrumentation and measurement methods, and will present a first set of cases selected for stability analysis and transition evaluation. Various tools for stability analysis and transition predictions will be tested, from local stability theory with the envelope methods to non-local theories taking into account curvature and non-local effects, based on the parabolized stability equations or on a multiple scale approach for compressible flows.*

1 INTRODUCTION

The objective of a fifty percent reduction in aircraft fuel consumption, (together with eighty percent reduction in nitrogen oxides and 6 dB in perceived noise level), was introduced in 2001 by the European Union in the 'Vision 2020' for European Aeronautics, and requires breakthrough achievements related to drag reduction and propulsion efficiency. Similar trends may be expected in other parts of the world. Laminar flow technology may be seen as a promising candidate to contribute to these objectives, as the extended laminar flow region allows a strong decrease in friction drag. Laminar flow may be attained by shape optimisation (Natural Laminar Flow, or NLF), possibly associated with wall suction (Hybrid Laminar Flow Control, HLFC). Another line of research dealing with 'long endurance UAVs' also calls for a large reduction of total drag, including friction drag.

In the past, a number of flight demonstrators were successfully used both in the USA[1,2] and in Europe (Falcon 50[3] and 900, ATTAS, Fokker 100[4], Airbus A320[5]). Flight tests were selected as they allow full system demonstration at flight Reynolds numbers which are not attainable in conventional wind tunnels: maximum chord Reynolds number Re_C in a transition test in transonic flow in the ONERA S1Ma facility is about 15×10^6. On the other hand, such flight tests are much too expensive to allow for extensive parametric exploration and optimization.

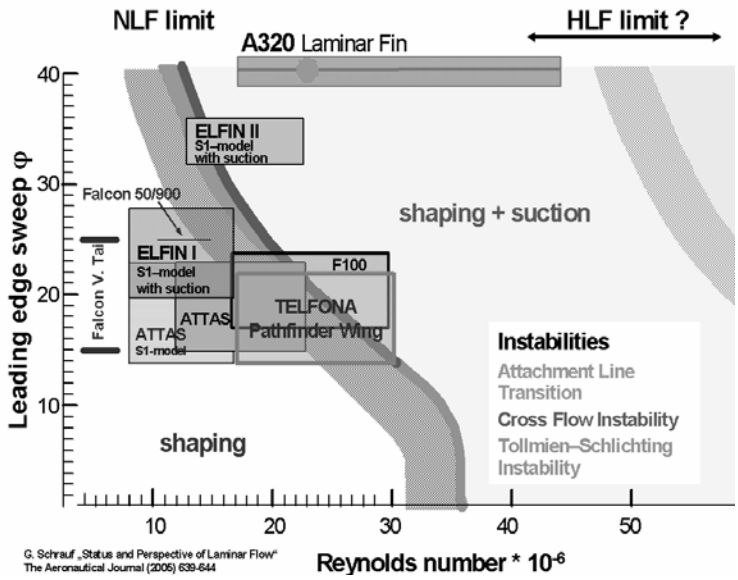

Figure 1. Various wind tunnel and Flight Laminar wing experiments in a Reynolds number versus Sweep angle domain[6].

As the ETW cryogenic wind tunnel allows chord Reynolds numbers up to $Re_C = 30\times10^6$ by combining cryogenic temperatures (down to 115 K) and pressurization (up to 3 bar), the TELFONA European Research Project, led by Airbus, was launched to demonstrate the use of ETW for NLF wing design at large Reynolds numbers. Two main steps were defined, first the design and test of a 'calibration' model, to be followed by a more realistic transport aircraft model. This paper is dedicated to the first of these two models, called 'Pathfinder', which was especially designed in order to allow the calibration of the Wind Tunnel transition N-factors, in the frame of the e^N method[7,8], at large values of chord Reynolds number typical of testing in ETW. Figure 1 shows the ranges in Reynolds number versus sweep angles of various wind tunnels and flight tests, with the corresponding expected domain for the Pathfinder experiment.

The first part of the paper will deal, as in a previous version[9], with model design and specific instrumentation for transition detection in cryogenic conditions. Then, typical experimental results will be presented, followed by stability analysis and N-factor correlations for this model in ETW. Stability analysis was applied after the tests in order

to ‘calibrate’ the various tools currently used by research laboratories and Industry in Europe, including simplified database, local linear and non-local linear stability approaches. Examples of numerical results obtained by the project partners will be compared to the experiments, and the physical meaning of the N-factor values obtained will be discussed.

2 MODEL DESIGN

The full span Pathfinder model was designed by CIRA, DLR, Airbus and ONERA for the calibration of transition measurements in ETW. A simple swept planform with a low taper and 18 deg. sweep angle was selected. This leading edge sweep was chosen knowing that additional side slip would allow the examination of the effect of sweep angle variation on leading edge crossflow transition.

The wing section was then determined such that the N-factor evolution coming out of stability calculation would grow linearly over the longest possible chordwise distance. In a first step, candidate aerofoil sections were designed independently by the three partners, each using their preferred design toolsets. CIRA used a boundary layer coupled Euler method with an ONERA transition prediction method. DLR used an inverse design procedure based on the FLOWer code, whilst ONERA preferred to modify the existing Fokker 100 glove aerofoil using the elsA code.

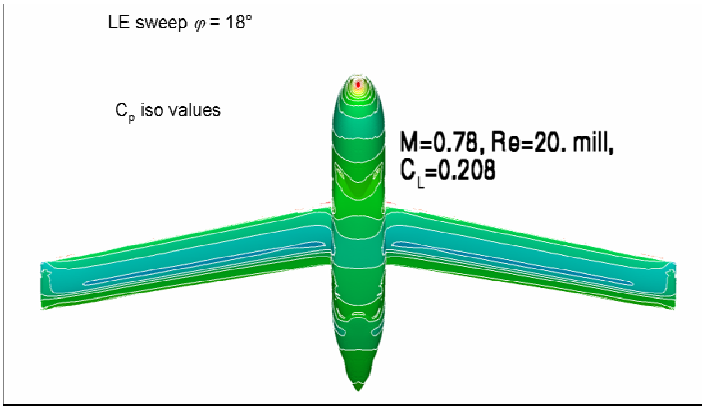

Figure 2. View of the model with pressure distributions.

The three proposed aerofoils were then reviewed, and the DLR LV5 aerofoil was finally selected. This LV5 aerofoil was derived from an ATTAS laminar glove section and modified for the higher Mach number (M=0.78) flow condition. In the following phase, the final wing design was conducted in the presence of a prescribed fuselage geometry with belly fairing from an existing ETW model.

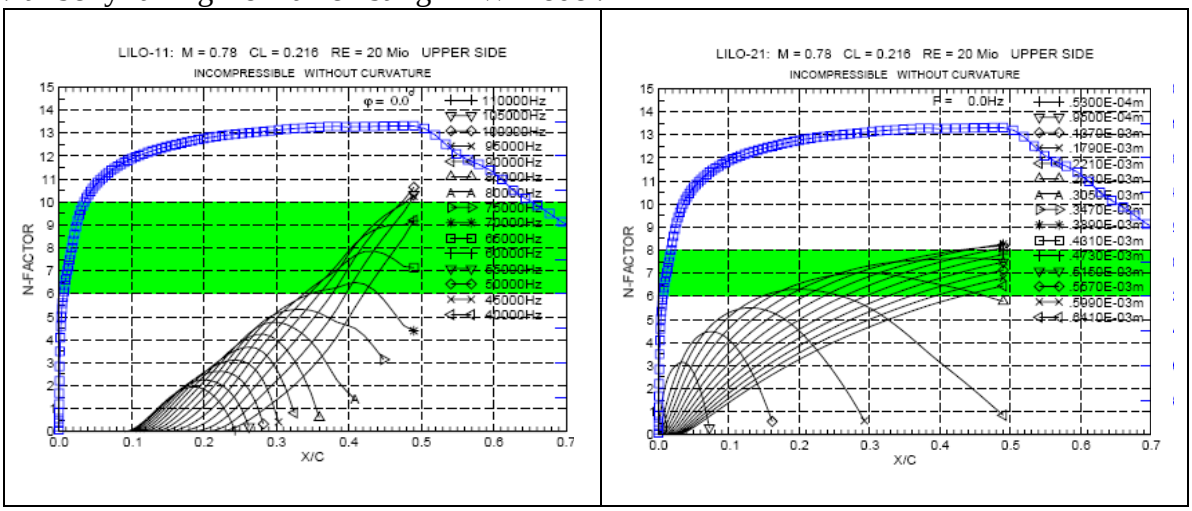

Figure 3. Pre test stability computations at design conditions

The DLR inverse design method[10] for transonic wings was applied in order to obtain parallel isobars from 30 to 70 % of span for the design point M=0.78, Re=20×10^6, $C_L = 0.216$, as shown in figure 2. While at the design point the designed wing has a constant pressure distribution in the region of interest, analysis performed at off-design points showed that the spanwise variation of sectional pressure distributions is sufficiently weak. Therefore, for the Pathfinder wing, stability analysis based on either numerical or experimental data can be associated to a pressure distribution on a constant span section. Finally, Airbus analyzed the pressure distributions supplied by DLR for design and off-design conditions using linear stability theory in the LILO code[11].

Figure 4. View of the model with 2 patches of TSP on the upper side

A typical result from Airbus is shown in figure 3, where the N-factor based on incompressible constant wavevector direction ψ is used to evaluate Tollmien Schlichting (TS) growth, and N-factors based on incompressible constant spanwise wavenumber β^*, at zero frequency, are used to evaluate the growth of crossflow (CF) modes.

3 PRE-TESTS STABILITY COMPUTATIONS

Based on computed pressure distribution, a first numerical simulation of the experiments was conducted based on the final model geometry. The range of conditions covered by the wind tunnel was explored, resulting in typical N-factor curves as shown in figure 3.

Mach number	Lift coefficient	Sweep angle	Re_C (Millions)	TS	CF	Mixed
0.78	0.11	18°	20	1	1	
0.78	0.22	18°	20		1	1
0.78	0.33	18°	20		1	1
0.76	0.22	18°	20			1
0.80	0.22	18°	20		1	
0.78	0.11	14°	20	1		1
0.78	0.11	22°	20	1	1	
0.78	0.22	22°	20		2	
0.78	0.33	22°	20		2	
0.76	0.11	14°	20	1		
0.76	0.11	18°	20	2		
0.76	0.33	22°	20			1

Table 1. List of cases selected at the end of pre-test computations

On this figure, the isolated curve shows the pressure distribution, while the grouped curves are obtained on the left side with the constant ψ strategy for incompressible flow for frequencies between 11 and 40 kHz, and on the right side with the constant β^* strategy for stationary modes. These N-factor curves contribute to an envelope, visible on the figure, which is indeed almost linear with x/c distance, as required. These pre-test

computations indicated that more crossflow situations were to be expected, re-enforcing the interest for non zero side slip angle situations for generating TS cases. From the N-factor survey of the Pathfinder model performed in this pre-test stability analysis[12] twenty one flow conditions, given in table 1, were identified with interesting stability behavior for calibrating ETW. As indicated in the table, there are six TS, nine CF and five mixed cases with strong TS and CF amplification.

4 MEASUREMENT SYSTEMS FOR CRYOGENIC TRANSITION DETECTION

Two lines of pressure taps were installed on each wing, as well as patches, applied on both suction and pressure sides, of a two component cryogenic temperature-sensitive paint (cryoTSP). This paint[13] is composed of two kinds of luminescing molecules incorporated into a transparent binder. These molecules re-emit light with an intensity depending on temperature when excited by incident light in a given wavelength range. First, a "standard" molecule (Ruthenium-complex Ru) is used, which works in the range 100 K < T < 240 K. Best operating temperature for this molecule is around 180 K, because it then exhibits the best relation of sensitivity and brightness. The sensitivity for Ru decreases for T > 240 K, but with rapidly increasing signal to noise ratio (S/N) because of the much lower intensity. Highest sensitivity for the Ruthenium is around 240 K, but with 20 times less intensity compared to 160 K, for example, making exposure times extremely long (despite the high signal to noise ratio). In order to improve the cryoTSP response for the "warm" temperatures (240 K < T < ambient), DLR (Y. Egami) included a second molecule (Europium complex) into the original paint (developed by Jaxa), in addition to the Ruthenium. This Europium complex shows good sensitivity and high brightness for the warmer temperatures, for which the Ruthenium complex becomes less adapted. The selection of one or the other molecule is determined by the wavelength of the incident light. A Xenon UV-flashlight excites the Europium and not the Ruthenium. Therefore UV light, and Europium, is used in the range 240 K < T < ambient. When performing transition detection at cold temperatures, the Ruthenium molecule is selected by changing the excitation light from UV to blue range (around 455nm), using light emitting diode (LED) illumination. Europium, on the other hand, is not excitable by the LEDs.

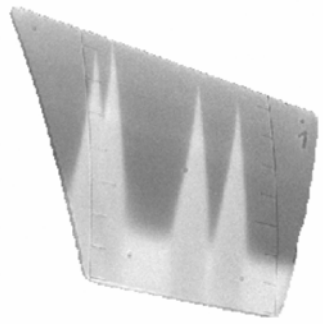

Figure 5. Example of transition detection at a low Reynolds number of 7 million.

The molecules then emit red light with temperature-dependent intensity, which is recorded by a number of CCD cameras. The wall temperature difference between laminar and turbulent boundary layer can thus be detected by the cryoTSP method, allowing the visualization of the boundary layer transition. On the pathfinder model, shown in figure 4, very thin, custom-built pockets on the wing's upper and lower surfaces have been sprayed with the TSP and polished to a very smooth surface, in-line with the metallic surface adjacent to the TSP areas. These four patches may be identified using the number visible on one corner (see figure 5): 1 and 2 for the upper side, 3 and 4 for the lower side, 1 and 3 corresponding to the right wing.

In order to increase spatial variations of temperature on the model wall, linked to the boundary layer nature, a thermal imbalance is required. This is obtained by changing the flow temperature in a stepwise manner, by about ten degrees. Following this change, a

number of TSP images are recorded. Pressure measurements are realized before and after the TSP recording, in order to detect accidental changes during the test. An example of temperature visualization at 7 million Reynolds number is shown in figure 5, with the flow coming from the top. The image on figure 5 is a raw image with laminar region in grey and turbulent ones in white. Reversed contrast is used on fully processed images shown in the rest of the paper.

Test number, Cp	Test number, TSP	Mach	ReC (millions)	T (K)	CL
P079	P080	0.78	20	175	0
P081	P085	0.78	20	175	0.1
P086	P087	0.78	20	175	0.21
P088	P089	0.78	20	175	0.32
P090	P091	0.78	20	175	0.4
P092	P093	0.78	20	175	0.5

Table 2. Cases selected for stability analysis

5 WIND TUNNEL TESTS

Three short experimental test campaigns were realized with the Pathfinder model, each improving the handling of the wind tunnel, the model and its instrumentation for these difficult measurements. Unusual precautions proved necessary in order to reduce to a minimum the presence of small particles in the flow, those particles causing

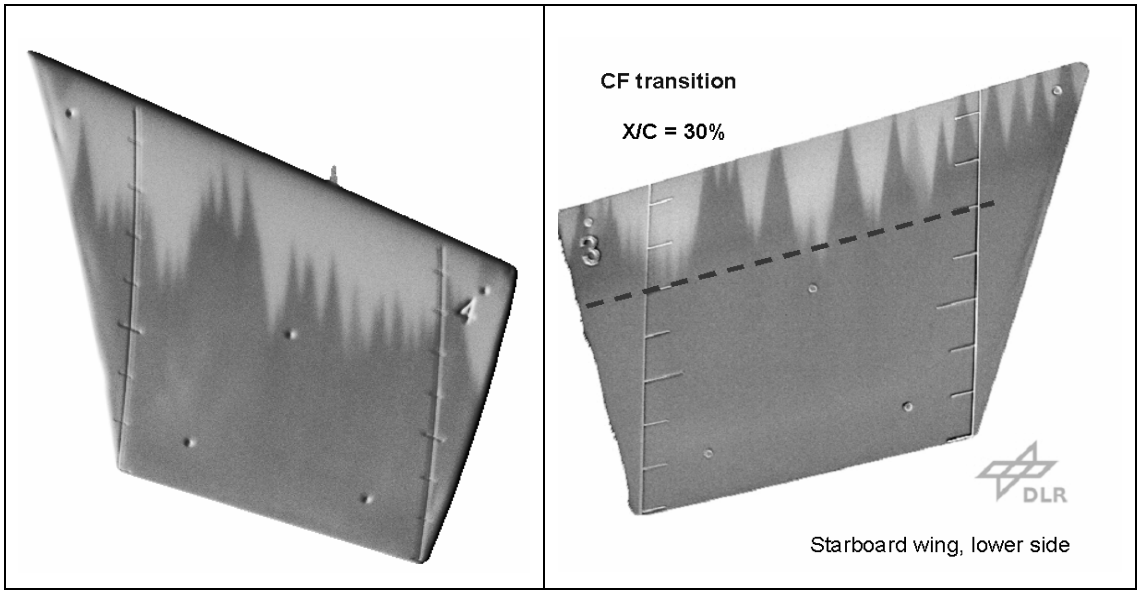

Figure 6. Typical TSP images at Re_C = 10 (left) and 20 (right) million.

turbulent wedges when impacting near the attachment line of the wing. Enquiry into the nature of these particles proved that there was no humidity, i.e. no ice particles in the nitrogen flow. This allowed very low temperatures, of about 115 K, to be used. Typical results for the lower side are shown on figure 6 at chord Reynolds numbers of 10 and 20 million. The right image, showing crossflow transition, was obtained at Mach 0.78 with a static temperature of 156 K and with a side slip angle of 4 deg. The left image, also CF, was obtained at the same Mach number, a temperature of 175 K, and a larger static pressure close to 3 bar. In the course of these experiments, the Reynolds number range 7 to 23×10^6 was explored. It was observed that below Reynolds number 15×10^6 transition would in general be imposed either by the shock, on the upper side, or by the pressure recompression on the lower side. In those cases, the experiment would not provide

interesting results with regard to the calibration of the N-factor methods. The most interesting results were obtained at 20×10^6 and are summarized in table 2.

The four cases selected for further analysis are highlighted in the table. As a concluding remark, it should be noted that although this experiment was difficult, ETW produced a very large amount of results in a very short timeframe.

6 ANALYSIS OF RESULTS

Raw measurements obtained after the experiments required some post treatment before further analysis. Raw TSP images may be improved by averaging and numerical treatments. Figure 5 gives an example of raw data obtained at Reynolds number 7×10^6. The images on figure 6 are typical of the final stage of treatment. On such small models, the number of pressure taps is always kept to a minimum, because of space constraints. Careful treatment of the pressure distribution is always necessary, and was conducted in this case by Airbus[15], who determined the location of the attachment line and the effective sweep, and produced sets of interpolated pressure coefficients C_p in formats adapted for boundary layer computation, as illustrated in figure 7. Airbus also performed boundary layer calculations and provided boundary layer data to the other partners involved. In the following, cases are identified with their test number, followed by three letters. The first one (P,S) determines which wing is used, port or starboard. The second (I,O) indicates which section is considered, and the third (U,L) indicates which side is considered, upper or lower.

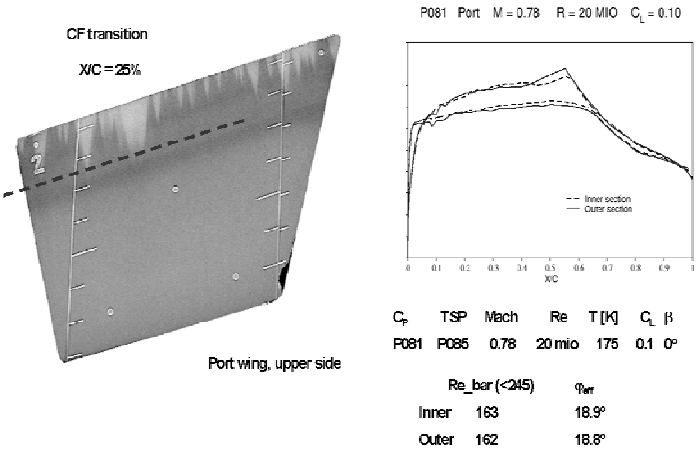

Figure 7. Typical dataset for analysis of experimental results.

6.1 Local Stability Theory

Although more sophisticated approaches are now available for computing the growth of instabilities in boundary layer flows, local theory is still considered a relevant engineering tool for two reasons: (1)-scatter of transition N-factors from ATTAS and Fokker 100 flight experiments showed no statistical improvement when comparing local theory with linear PSE, and (2)-local stability calculation can be made fast and robust enough as to become a component in industrial CFD tool, allowing an automatic treatment of transition prediction. Presently, it is accepted that non-local stability theory allows a better evaluation of the physics controlling instabilities, and that non-linear stability is a powerful tool when dealing with complex issues like flow control.

When dealing with the e^N transition prediction approach applied to the local stability of 3D flows, there exist a number of methods based on different N-factor integration strategies. Airbus (G. Schrauf) advocates for the so-called N_{TS}/N_{CF} approach, in which N_{TS} is obtained by using the constant ψ strategy at frequencies covering the complete range of unstable waves, and N_{CF} is obtained by considering only stationary

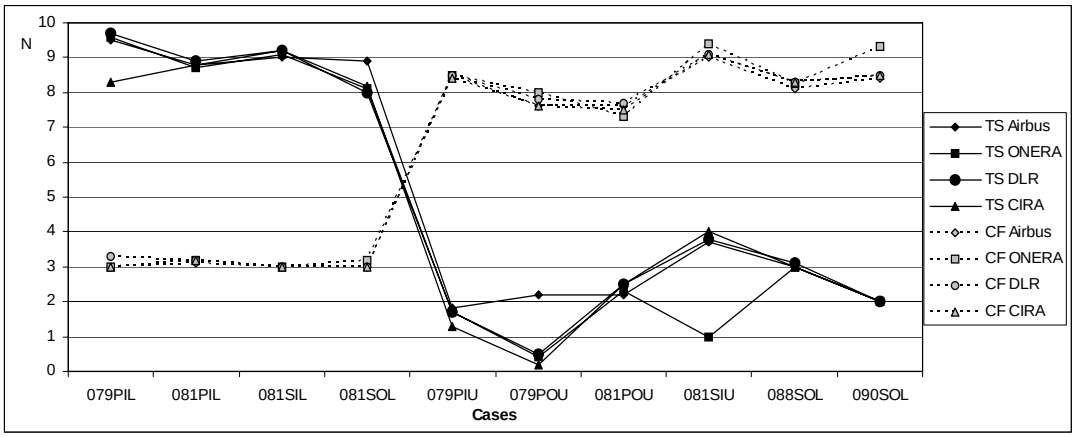

Figure 8. Local stability results obtained with the incompressible N_{CF}/N_{TS} method

instabilities, using either the constant wavelength strategy or the constant spanwise wavenumber β^* strategy.

In this approach, the N-factors are computed considering only incompressible stability equations, even though the cases of interest are transonic. A robust and efficient code, LILO, has been developed based on this method, and is integrated into a compressible boundary layer code. Results obtained with this approach are presented on figure 8, with TS cases to the right and CF cases to the left, and show the typical crossing of N_{TS} and N_{CF} curves between the two types of transition. ONERA used the in-house code CASTET[16], DLR and Airbus used LILO[11], and CIRA an improved version of COSAL[17].

Both N_{TS} and N_{CF} may also be computed with compressible local stability theory. Another strategy commonly used is the envelope method, in which the amplification rate belonging to the most unstable solution is selected and integrated to form an N-factor curve. Results of local compressible stability theory from ONERA, DLR, and CIRA are presented in figure 9, based on both the N_{CF}/N_{TS} and the envelope methods. CF N-factors varies from 8 to 10 for crossflow cases, an acceptable range. Envelope N-factors are close to 12 for TS cases, but varies from 13 to 17 for crossflow cases, showing in this case quite a large dispersion of results.

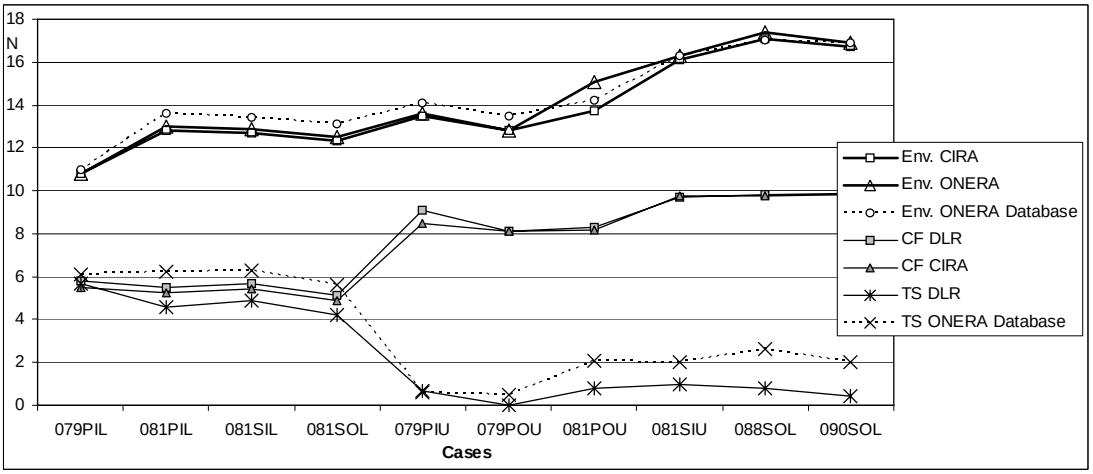

Figure 9 : Compressible local stability results

6.2 The Database Method

A number of models have been created at ONERA to allow rapid estimation of the amplification rates corresponding to local theory[18]. This database method allows the definition of longitudinal and crossflow N-factors similar to what is done in the N_{TS}/N_{CF} strategy, as well as an estimation of the envelope N-factor. In this case again, the method is robust and fast, and is integrated into a boundary layer code for transition prediction. Numerical results are shown in figure 9, compared to the equivalent local stability results. Two main differences in the definitions of N-factors have here a visible effect. First, the database is applicable to compressible flows, which explains the difference in N_{TS} values for TS cases. Second, database N_{CF} are defined using an envelope method at zero frequency, instead of a constant spanwise wavenumber strategy, which explains the vertical shift between the two curves. Nevertheless, a similar crossover is observed as in the previous figure, and the N_{CF}/N_{TS} based on the database method can also be used for transition prediction, at a fraction of the computing time necessary for any exact method.

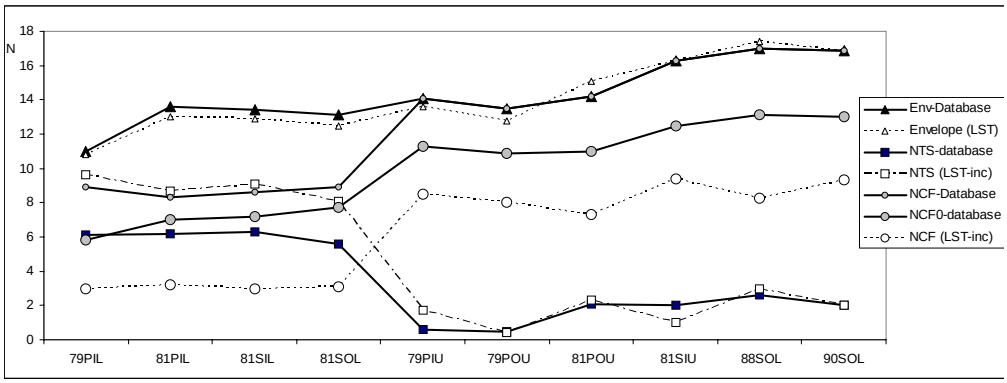

Figure 10. Comparing local stability results with ONERA database results.

6.3 Non-Local Stability Theories

Local theories do not take into account the rate of change of the mean flow. As curvature terms are of same order as non-local terms, they should also be excluded. Non-local theories, either Parabolized Stability Equations (PSE) or the multiple scale approach, include the missing terms. PSE codes from FOI and DLR (the NOLOT code[18,20]), and a code based on the multiple scale approach from CIRA (the NOLLI code[21]) were also used to analyze the Pathfinder data.

All these methods assume no variations of the mean flow in the spanwise direction,

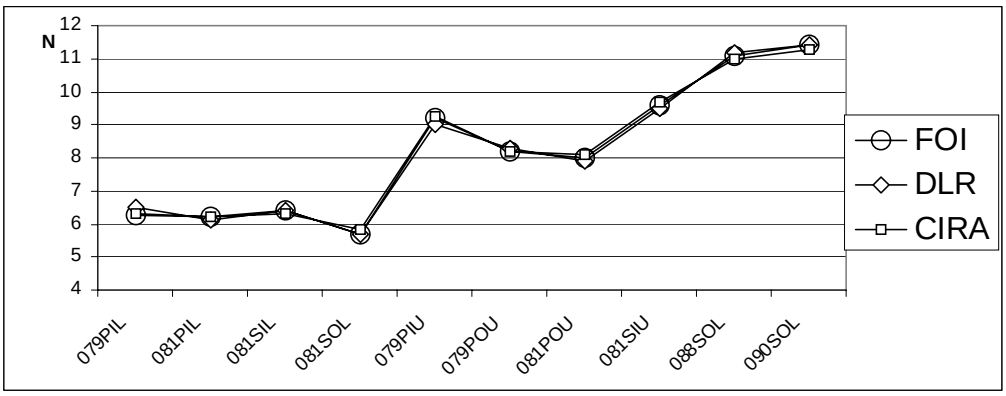

Figure 11. Non-local stability results (compressible with curvature)

and are well adapted to consider swept wings. As in local theory, N_{CF} values may be obtained by considering only stationary disturbances, by imposing f=0 Hz. The envelope of envelope method, more time consuming, requires N-factor computations for all unstable spanwise wavenumbers and frequencies.

Examples of envelope of envelope results are presented in figure 11, obtained with two different formulations. An excellent agreement is observed between CIRA, with the NOLLI code, and DLR and FOI using two versions of NOLOT. The results obtained here show again that a different value of transition N-factor must be used when dealing with TS (N close to 6.2) or with CF (N close to 9.5) cases.

		Database	Incomp LST	Comp LST	Non-local, comp + curvature
Envelope	TS	**12.8**		**12.3**	
	CF	**15.3**		**15**	
N_β (env of env)	TS	8.7		5.5	**6.2**
	CF	**15.3**		**9.15**	**9.5**
N_β (f=0)	TS	6.9	3.1	0	0
	CF	**12**	**8.4**	7.8	7
N_ψ (ψ=0)	TS	**6**	**9**	**4.6**	
	CF	1.6	2.4	0.5	

Table 3 : Transition N-factors obtained with various strategies and methods

Since a unique N-factor is here computed, there is no a-priori information for deciding which threshold should be used, TS or CF. Computation of a zero frequency N-factor may allow to identify CF and TS cases, so that the e^N approach may also be effectively used based on non-local computations.

7 DISCUSSION ON THE VALUES OF N-FACTORS

The previous sections may convey the impression that a confusing number of methods can be used for the computation of N-factors, as summarized on table 3. This table shows the various mean N-factors at transition, obtained from the previously presented results. Lines correspond to strategies, while columns show the various levels of modelling, from the database to non-local codes. For each strategy, TS and CF cases have been separated. Bold numbers show the most significant values.

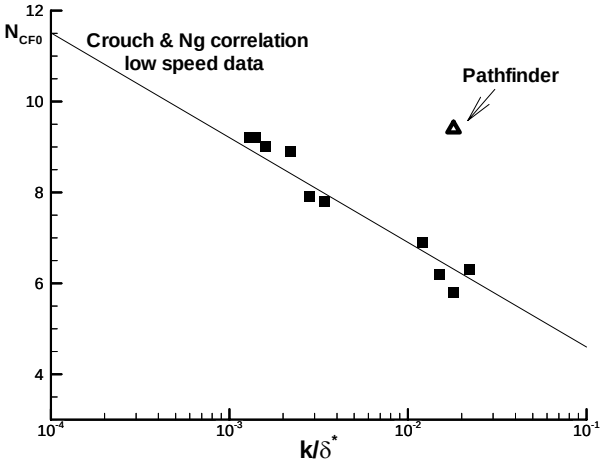

Figure 12. Correlation between surface roughness and crossflow N-factors

There are in fact two main families, one based on a single value for transition prediction and the second using two separate N-factors, one for TS and one for CF. In the first family, the envelope method is the most usual, and the envelope of envelope N_β is generally preferred in the context of non-local theory. In the second family, the constant spanwise wavenumber strategy is usually selected for evaluating crossflow, while a constant wavevector direction strategy is used for TS. Looking at table 3, it can be seen that the

database envelope N-factors are very close to compressible LST, while N_{TS}/N_{CF} are rather different (because their definitions are then different, N_{TS} is computed including oblique waves and N_{CF} (f=0) is obtained using an envelope method at zero frequency). Incompressible LST, considering only stationary waves for crossflow and ψ=0 for TS, is at present the Airbus preferred approach because it provides quite good correlations when considering flight test results.

Compressible N-factors are equal to 6 (database) and 6.2 (non-local approach) for the four TS cases. These values correspond to a turbulence level of about 0.20 % based on Mack's law (N_{TRANS} = -8.43-2.4ln(Tu)). But the TS instabilities are observed in a frequency range 15 kHz < f < 100 kHz, far above the frequencies contributing most to the global turbulence level (up to a few kHz). Concerning crossflow, the other six cases produce an average N_{CF} of 8.4 for stationary vortices, based on incompressible LST, similar to the level observed in the Fokker 100 flight tests. According to the correlations proposed by Crouch and Ng[22], based on low speed flow results from Saric, the value of N_{CF} at transition is related to the height of distributed roughness (characterized by a RMS roughness height k_{RMS}) in the region of the critical point, close to the attachment line. On the Pathfinder model, the very thin boundary layer increases sensitivity to roughness, while a careful preparation resulted in a smooth surface, with $k_{RMS} < 0.1$ μm. Results on figure 12 compares the low speed correlation proposed by Crouch and Ng with a typical Pathfinder transonic result. As flow regimes are very different, it is not surprising to see the Pathfinder point well above low speed points. That N-factors should in fact be larger was indeed expected, as similar correlation was also considered for supersonic flows[23], and produced another line clearly above the low speed one. No other point was found available in open literature for transonic conditions.

8 CONCLUSIONS

Careful design of the Pathfinder model was conducted in order to allow the calibration of ETW in a large range of Reynolds numbers. The goal of this calibration is to determine transition N-factors for both crossflow (CF) and longitudinal (TS) instabilities, knowing that TS N-factors are mostly related to non-stationary disturbances caused e.g. by free-stream turbulence or noise, while CF N-factors are related to the wall surface quality in the region of the leading edge.

Experimental difficulties reduced the Reynolds number range effectively useful for correlation, and the number of tests that could be analysed. The flow over the model showed to be too stable up to about $Re_C = 15\times10^6$ to obtain a transition location function of the expected instabilities, and finally the range explored went from about 15 to 23×10^6. Nevertheless, the experiments confirm the possibility to observe laminar-turbulent transition up to $Re_C = 23\times10^6$ in ETW. Experience has been gained on the best running conditions in ETW for large Reynolds number transition experiment, and the TSP imaging system was proved to be an efficient method for transition detection in a wide range of temperatures, from ambient to cryogenic. Finally, N-factor calibration of ETW has been achieved in a rather narrow range of conditions

Concerning transition prediction, it can be stated that:

- The classical envelope method, with a single N-factor, does not produce a single reliable correlation for this type of configuration. Separate transition N-factor values must be used for TS and crossflow cases. The use of two N-factors, one associated with TS transition and the other with crossflow, appears to be slightly more robust. On the other hand, the rather large dispersion observed for CF cases, using the envelope method but also observed with the non-local computation, may result from the relatively small number of tests analysed here.

- The proposed way of considering incompressible stability theory and computing the crossflow N-factor with the constant β^* strategy for stationary disturbances should be improved. This approach has a tendency to produce N-factor curves with large values close to the leading edge, decreasing to lower values at transition (so-called pathological cases). Other definitions for N_{CF} could be based on a zero frequency envelope, or using the constant β^* strategy for stationary disturbances in non-local theory. These two definitions have the effect of reducing considerably the number of pathological cases.

There is hope in a near future to complement the analysis based on measured pressure distributions with CFD based analysis, using Navier Stokes computed mean flows[24]. As a final comment, a set of test cases will be made available for validation of stability codes, derived from those obtained in the course of this work, with information and datasets allowing cross validation of stability computations in the frame of local and non-local theories.

ACKNOWLEDGMENTS

The work presented in this paper was part of the research project TELFONA, performed under contract No. AST4-CT-2005-516109, financed by the European Union. Thanks to Donato de Rosa (CIRA), who produced the final NOLLY results, Winfried Kuhn (Airbus) who contributed to the test, Jean-Pierre Archambaud (ONERA) who remained involved for the complete duration of the TELFONA project, and the ETW team of test engineers and technicians who prepared the model.

REFERENCES

[1]Collier, F.S., "An Overview of Recent Subsonic Laminar Flow Control Flight Experiments", AIAA Paper 93-2987, 1993

[2]Braslow, A.L., "A History of Suction-type control with Emphasis on Flight Research", Monograph in Aerospace History, No. 13, 1999

[3]Bulgubure, C. and Arnal, D., "Dassault Falcon 50 laminar flow flight demonstrator", First European Forum on Laminar Flow Technology, Hamburg, Germany, March 1992

[4]Schrauf, G., Perraud, J., Vitiello, D. and Lam, F., "Comparison of Boundary Layer Transition Predictions using Flight Test Data" Journal of Aircraft Vol. 35, No. 6, 1998, pp. 891-897, doi: 10.2514/2.2409

[5]Schrauf, G., "Large-scale laminar flow tests evaluated with linear stability theory", AIAA Paper 2001-2444

[6]Schrauf, G., "Status and perspectives of laminar flow", The Aeronautical Journal, Vol. 109, No. 1102, December 2005, pp. 539-644

[7]Smith, A.M.O., and Gamberoni, N., "Transition, pressure gradient and stability theory" - Douglas Aircraft Co, Rept. ES 26388, El Segundo, California (1956)

[8]Van Ingen, J., "A suggested semi-empirical method for the calculation of the boundary layer transition region" - Univ. of Techn., Dept of Aero. Eng., Rept. UTH-74, Delft (1956)

[9]Perraud, J., Archambaud, J.-P., Schrauf, G., Donelli, R., Hanifi, A., Quest, J., Streit, T., Hein, S., Fey, U. and Egami, Y., "Transonic High Reynolds Number Transition Experiments in the ETW Cryogenic Wind Tunnel", AIAA Paper 2010-1300, 48th AIAA Aerospace Science Meeting, Jan 2010, Orlando, Florida

[10]Bartelheimer, W., "Ein Entwurfsverfahren für Tragflügel in transsonischer Strömung, Dissertation TU-Braunschweig, DLR FB 96-30,199.

[11]Schrauf, G., "LILO 2.1 – Users' Guide and Tutorial", GSSC Technical Report, July 2006

[12]Schrauf, G., Horstmann, K. H. and Streit, T., "The Telfona Pathfinder Wing for the Calibration of the ETW Wind Tunnel" Proceedings of the 1st CEAS European Air and Space Conference, 10-13 September, Berlin, 2007.

[13]Fey, U., Egami, Y. and Engler, R. H., "High Reynolds number transition detection by means of Temperature Sensitive Paint", AIAA Paper 2006-0514 (2006).

[14]Fey, U., Konrath, R., , Kirmse, T., Ahlefeldt, T., Kompenhans, J. and Egami, Y., "Advanced Measurement Techniques for High Reynolds Number Testing in Cryogenic Wind Tunnels", AIAA Paper 2010-1302 (2010)

[15]Schrauf, G., Horstmann, K. H., Streit, T., Perraud, J. and Donelli, R., "The Telfona Pathfinder Wing for the Calibration of the ETW Wind Tunnel" KATnet II Conference on Key Aerodynamic Technologies, 12-14 May, Bremen, 2009

[16]Laburthe, F., "Problème de stabilité linéaire et prévision de la transition dans des configurations tridimensionnelles, incompressibles et compressibles", Thèse de Doctorat Sup'Aéro, Toulouse, Dec. 1992

[17]Malik, M. R., "COSAL – A black-box compressible stability analysis code for transition prediction in three-dimensional boundary layer", NASA CR-165925, 1982.

[18]Perraud, J., Arnal, D., Casalis, G. and Donelli R., "Automatic transition Predictions using Simplified Methods", AIAA Journal, Vol. 47, No. 11, Nov. 2009, pp 2676-2684, doi: 10.2514/1.42990

[19]Hein, S., Bertolotti, F. P., Simen, M., Hanifi, A. and Henningson, D., "Linear non-local instability analysis – the linear NOLOT code –. DLR Internal Report IB 223-94 A56, 1994

[20]Hanifi, A., Henningson, D., Hein, S., Bertolotti, F. P. and Simen, M., "Linear non-local instability analysis – the linear NOLOT code –. FFA TN 1994-54, 1994

[21]De Matteis, P., Donelli, R. and Luchini, R. S., "Application of the ray tracing theory to the stability analysis of three-dimensional incompressible boundary layers", XIII AIDAA Conference, Rome, Italy, 1995

[22]Crouch, J.D., and Ng, L.L., "Variable N-factor method for transition prediction in three-dimensional boundary layers", AIAA Journal, Vol. 38, No. 2, pp 211-216, 2000

[23]Archambaud, J.-P., Arnal, D., Séraudie, A., Carrier, G. and Louis, F., "Calibration of the e^N method for transition prediction in 2D and 3D supersonic flows", CEAS Katnet Conference on Key Aerodynamic Technologies, Bremen, Germany, 20-22 juin 2005

[24]Streit, T., Schrauf, G., Salah El Din, I., Cella, U., Fey, U. and Egami, Y., "The TELFONA Pathfinder model, a second look", ECCOMAS CFD 2010, Paper 1787, Lisbon, June 2010